



Organic Carbon Linkage with Soil Colloidal Phosphorus at Regional and Field Scales: Insights from Size Fractionation of Fine Particles

Li, Fayong; Zhang, Qian; Klumpp, Erwin; Bol, Roland; Nischwitz, Volker; Ge, Zhuang; Liang, Xinqiang

Environmental Science and Technology

DOI:

[10.1021/acs.est.0c07709](https://doi.org/10.1021/acs.est.0c07709)

Published: 04/05/2021

Peer reviewed version

[Cyswllt i'r cyhoeddiad / Link to publication](#)

Dyfyniad o'r fersiwn a gyhoeddwyd / Citation for published version (APA):

Li, F., Zhang, Q., Klumpp, E., Bol, R., Nischwitz, V., Ge, Z., & Liang, X. (2021). Organic Carbon Linkage with Soil Colloidal Phosphorus at Regional and Field Scales: Insights from Size Fractionation of Fine Particles. *Environmental Science and Technology*, 55(9), 5815-5825. <https://doi.org/10.1021/acs.est.0c07709>

Hawliau Cyffredinol / General rights

Copyright and moral rights for the publications made accessible in the public portal are retained by the authors and/or other copyright owners and it is a condition of accessing publications that users recognise and abide by the legal requirements associated with these rights.

- Users may download and print one copy of any publication from the public portal for the purpose of private study or research.
- You may not further distribute the material or use it for any profit-making activity or commercial gain
- You may freely distribute the URL identifying the publication in the public portal ?

Take down policy

If you believe that this document breaches copyright please contact us providing details, and we will remove access to the work immediately and investigate your claim.

1 **Organic carbon linkage with soil colloidal phosphorus at regional and field**
2 **scales: insights from size fractionation of fine particles**

3 Fayong Li^{1, 2#}, Qian Zhang^{3, 4#}, Erwin Klumpp³, Roland Bol^{3, 5}, Volker Nischwitz⁶, Zhuang Ge⁷,
4 Xinqiang Liang^{1*}

5 ¹ Key Laboratory of Environment Remediation and Ecological Health, Ministry of Education,
6 College of Environmental and Resources Sciences, Zhejiang University, Hangzhou 310058, China

7 ² College of Water Resources and Architectural Engineering, Tarim University, Xinjiang 843300,
8 China

9 ³ Institute of Bio- and Geosciences, Agrosphere (IBG-3), Forschungszentrum Jülich GmbH, 52425,
10 Jülich, Germany

11 ⁴ Institute for Environmental Research, Biology 5, RWTH Aachen University, Worringerweg 1,
12 52074 Aachen, Germany

13 ⁵ School of Natural Sciences, Environment Centre Wales, Bangor University, Bangor, LL57 2UW,
14 U.K.

15 ⁶ Central Institute for Engineering, Electronics and Analytics, Analytics (ZEA-3),
16 Forschungszentrum Juelich, 52425 Juelich, Germany

17 ⁷ Northeast Key Laboratory of Conservation and Improvement of Cultivated Land (Shenyang),
18 Ministry of Agriculture, Shenyang Agricultural University, Shenyang, Liaoning 110866, China

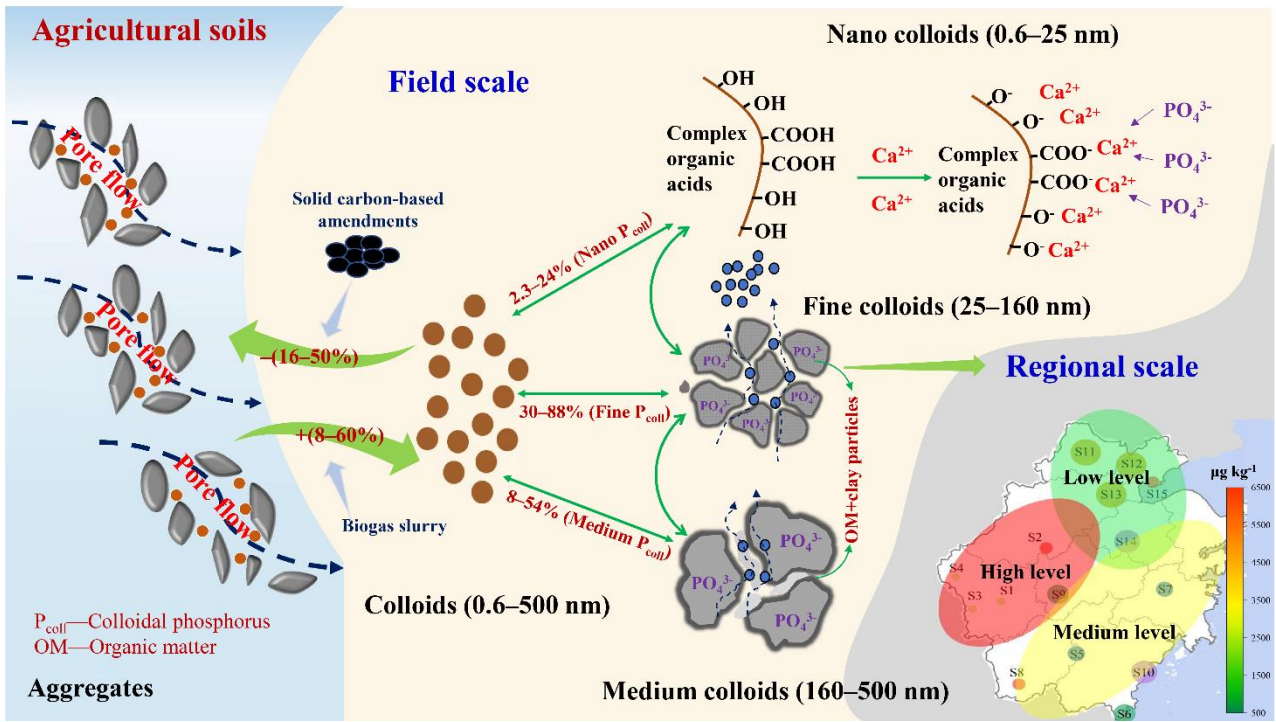
19 #These authors are co-first authors and contributed equally to this work

20 *Corresponding author: (liang410@zju.edu.cn; Tel & fax: 86-0571- 88982809)

21

22 **ABSTRACT:** Nano and colloidal particles (1–1000 nm) play important roles in phosphorus (P)
23 migration and loss from agricultural soils; however, little is known about their relative distribution
24 in arable crop soils under varying agricultural geo-landscapes at the regional scale. Surface soils (0–
25 20 cm depth) were collected from 15 agricultural fields, including two sites with different carbon
26 input strategies, in Zhejiang Province, China, and water-dispersible nano colloids (0.6–25 nm), fine
27 colloids (25–160 nm), and medium colloids (160–500 nm) were separated and analyzed using
28 Asymmetrical Flow Field Flow Fractionation (AF4) technique. Three levels of fine-colloidal P
29 content (3583–6142, 859–2612, and 514–653 $\mu\text{g kg}^{-1}$) were identified at the regional scale. The nano
30 colloidal fraction correlated with organic carbon (C_{org}) and calcium (Ca), and the fine colloidal
31 fraction with C_{org} , silicon (Si), aluminum (Al), and iron (Fe). Significant linear relationships existed
32 between colloidal P and C_{org} , Si, Al, Fe, Ca, and for nano-colloidal P with Ca. The organic carbon
33 controlled colloidal P saturation, which in turn affected the P carrier ability of colloids. Field-scale
34 organic carbon inputs did not change the overall morphological trends in size fractions of water
35 dispersible colloids. However, they significantly affected the peak concentration in each of the nano-,
36 fine- and medium-colloidal P fractions. Application of chemical fertilizer with carbon-based solid
37 manure and/or modified biochar reduced the soil nano-, fine- and medium-colloidal P content by
38 30–40%; however, application of chemical fertilizer with biogas slurry boosted colloidal P formation.
39 This study provides a deep and novel understanding of the forms and composition of colloidal P in
40 agricultural soils and highlights their spatial regulation by soil characteristics and carbon inputs.

41 **Keywords:** organic carbon; nano-colloidal phosphorus; colloidal phosphorus; Asymmetric Flow
42 Field-Flow Fractionation; biochar; regional scale; field scale



45 ■ INTRODUCTION

46 Loss of soil phosphorus (P) from agricultural fields has long been a global challenge, and is one of
47 the main factors responsible for the eutrophication of rivers and lakes in southern China^{1,2}. However,
48 the formation, distribution, and migration mechanisms of P in agricultural soils remain inadequately
49 understood, which presents great difficulties in source control mitigation where P is present as a
50 diffuse and non-point pollution source³. Previous studies suggest that the majority of P in soil exists
51 as larger-sized particulate and conventionally dissolved P, which are usually distinguished using a
52 0.45 μm filter membrane^{4,5}. However, this consideration neglects the important role of colloidal P
53 ($\sim 1\text{--}1000$ nm) and its subfraction nano-colloidal P ($\sim 1\text{--}100$ nm) in the process of soil P transport.
54 In fact, colloidal P forms have special colloid-chemical properties^{6,7}, which are fundamentally
55 different from that of truly dissolved P. In general, colloidal size fractions like nano colloids ($\sim 1\text{--}$
56 100 nm), fine colloids ($\sim 100\text{--}200$ nm), and medium colloids ($\sim 200\text{--}500$ nm) have a large specific
57 surface area and are rich in charge density, and, thus, they can immobilize P and other compounds^{8,9}.
58 The colloidal P can potentially migrate faster than truly dissolved P due to the spatial exclusion and
59 electrostatic repulsion of the soil matrix¹⁰. Moreover, some studies have found that the P molecules
60 carried by colloids with low bioavailability and small particle size enhance migration ability and
61 contribute to the transport of soil P to external water bodies^{11–13}. Overall, the migration and
62 transformation of colloidal P in agricultural soil systems is of crucial environmental and ecological
63 significance.

64 Related studies in acid forest river systems have indicated that organic carbon (C_{org}), iron (Fe),
65 and aluminum (Al) may be the main binding elements of nano-, fine- and medium-colloidal P, and

66 that the elemental composition may vary with the specific location within or between rivers¹⁴⁻¹⁵.
67 However, detailed colloidal P fluxes remain almost blind spots in some areas of ecosystem research¹⁶.
68 In agricultural systems, colloidal carriers may be affected by farm management practices, such as
69 irrigation, fertilization, and land-use types^{12,17}. Compared to forest soils, agricultural soils usually
70 have lower organic matter, higher inorganic mineral contents, and relatively stable seasonal input
71 and outputs¹⁸. Therefore, the composition and morphology of the colloids in agricultural soils may
72 be very different from those in natural ecosystems, e.g., forest and steppe soils. The majority of
73 previous research on colloidal P in agricultural systems has focused on the whole colloidal size range
74 (1–1000 nm) and single, specific farm types¹⁷, and only few studies have separated nano-, fine- and
75 medium-colloidal P^{19,20}. The rarest studies are those that also provide specific nutrient compositions
76 of colloidal particle size ranges^{21,22}. The emergence of the Asymmetrical Flow Field Flow
77 Fractionation (AF4) technique enables us to separate and study nano-, fine- and medium-colloidal
78 P²³. As an important advantage of this technique, crude extracts of soil water dispersible colloids
79 can be analyzed with the only requirement that the upper particle size is limited to about 500 nm by
80 centrifugation. The composition of nano-, fine- and medium-colloidal P in stream waters and soils
81 has been explored using this technique^{24,20,25,26}.

82 Input of carbon-based fertilizers directly affects the forms, composition, and loss of P in
83 agricultural soils^{27,28}. Organic fertilizer (manures) usually contains a large amount of organic P,
84 which may increase the soil P level after being applied to the soil²⁹. However, it may also reduce the
85 release of soluble P and improve soil bacteria activity compared with chemical fertilizers^{2,30}.
86 Carbon-based biochar has recently been recommended as an amendment that effectively improves

87 soil physical and chemical conditions and increases crop productivity^{31–32}. However, biochar
88 contains a large amount of soluble P, which may increase the loss of soil P once applied to the soil³³.
89 Conversely, it is rich in pore structures, specific surface area, and functional groups, which may
90 have the potential to immobilize soil P^{33,34}. However, regardless of the type of fertilization, organic
91 carbon input will participate in the formation of soil colloidal particles after entering the soil,
92 whereby some may be adsorbed by the colloids, and some may have colloidal properties (i.e., high
93 molecular mass organic acids). At present, there are very few reports on the elemental compositions
94 and morphologies of soil colloidal P under different carbon input strategies.

95 Therefore, we collected soil samples covering typical agricultural ecosystems from 15 sites
96 throughout Zhejiang Province, China, to explore the influence of organic carbon and other soil
97 parameters on nano-, fine- and medium-colloidal P at the regional scale. At the field scale, two
98 experimental stations were established to evaluate the effects of different carbon input strategies on
99 the soil P forms, content, and loss potential. Soil samples were analyzed using AF4 coupled to
100 inductively coupled plasma-mass spectrometry (ICP–MS) and to an online organic carbon detector
101 (OCD). We hypothesized that, due to different formation mechanisms: i) At the regional scale,
102 specific distribution patterns of nano-, fine- and medium-colloidal P occur under different land-use
103 types, and organic carbon affects the ability of colloids and nanoparticles to bind P; ii) at the field
104 scale, chemical fertilizer will increase soil nano-, fine- and medium-colloidal P concentrations;
105 however, carbon inputs (including organic fertilizer and biogas slurry, with or without modified
106 biochar) will reduce the soil nano-colloidal and fine/medium-colloidal P contents.

107 ■ MATERIALS AND METHODS

108 **Site description and soil sampling.** Soil samples were taken from 15 representative sites (H1–
109 H5, M1–M5, and L1–L5) with different land-use types in Zhejiang Province (Figure S1), China,
110 which included 6 agricultural planting types with conventional fertilization regimes (Tables S1 and
111 S2), which were almost evenly distributed in the county-level administrative area of the region
112 (1,055,00 km², Figure S1). In each sampling site, three representative fields (three replicates) of the
113 same crop type were selected, and 10-kg topsoil samples (0–20 cm depth) were randomly collected
114 from 10–15 points of each field without regard to soil horizons using S-shaped sampling method³⁵
115 and then mixed to prepare a representative sample of the whole field. Samples were air-dried and
116 divided into two portions: One portion was ground through a 0.154-mm sieve for determining the
117 basic physical and chemical properties, and the other portion was carefully broken into small pieces
118 by hand and passed through an 8-mm sieve for separation of water-dispersible colloids (WDC) and
119 determination of colloidal fractions. All the soil samples were stored in sealed plastic bags and kept
120 at 4°C before analysis. Detailed descriptions of sites and soils are shown in Table S1.

121 In addition, two experimental crop rotation field stations were established as part of the study
122 (Figure S1), i.e., in Site 1 (double-season rice) and Site 2 (rice-wheat rotation). Three treatments
123 with the same P application rate and a control (CK) were applied at each site. The P application rates
124 were 68.8 kg P ha⁻¹ per year (two seasons) at Site 1 and 103.2 kg P ha⁻¹ per year (two seasons) at
125 Site 2. The treatments in Site 1 were: a) Control without fertilization (CK), b) Conventional
126 fertilization (chemical fertilizer, CF), c) Chemical fertilizer + organic fertilizer (sheep manure) (OF),
127 and d) Chemical fertilizer + organic fertilizer + modified rice straw biochar (OFSB). The treatments
128 in Site 2 were: e) Control without fertilization (CK), f) conventional fertilization (CF), g) Chemical

129 fertilizer + biogas slurry (BS), and h) Chemical fertilizer + biogas slurry + modified rice straw
130 biochar (BSSB). Each treatment was repeated three times with a total of 12 completely random plots
131 (33.3 m² per each). Physicochemical properties of modified biochar, organic fertilizer, and biogas
132 slurry are shown in Table S3. The specific nutrient contents of fertilizers and the fertilization
133 schedule are shown in Tables S4 and S5, respectively. Five soil samples from the 0–20 cm soil layer
134 in each plot were randomly collected after harvesting in the second season and were mixed into a 5-
135 kg sample, transported to the laboratory, air-dried, and again divided into two equal portions (i.e., as
136 for all main site samples). One portion was ground through a 0.154-mm sieve to determine basic
137 physical and chemical properties. The other portion was carefully broken into small pieces by hand
138 and passed through an 8-mm sieve for separation of WDC.

139 **Soil physical and chemical parameters.** Soil particle size distribution was determined using
140 the hydraulic method according to the international soil texture classification³⁶. Soil pH was
141 determined using a glass electrode pH meter (PHS-3C, Shanghai) at a solid-to-liquid ratio of 1:5.
142 Soil cation exchange capacity (CEC) was determined using ammonium acetate (12.5 mL 1 M
143 NH₄OAc, 2.5 g soil)³⁷. Samples were digested with H₂SO₄-HClO₄, and the total P contents were
144 determined using molybdenum blue colorimetric method³⁸. Soil total carbon (TC) and total nitrogen
145 (TN) were measured using an element analyzer (Elementar, Vario MAX CNS, Germany). The
146 bioavailable fraction of Fe, Al, and Ca was determined using an Inductively Coupled Plasma-Mass
147 Spectrometer (ICP-MS; Agilent 7500, Agilent Technologies, Japan) after extraction by 0.2 mol L⁻¹
148 oxalic acid (2.5 g soil, 50 mL oxalic acid)³⁹. Soil available P (Olsen P) was extracted with 0.5 M
149 NaHCO₃ (pH 8.5)⁴⁰ and analyzed using molybdenum blue colorimetry.

150 **Water dispersible colloids extraction.** The water-dispersible soil colloids were extracted by
151 the method of Sequaris and Lewandowski ⁴¹, which avoids the destruction of small aggregates in
152 soil²⁵, and mainly includes two procedures of shaking and sedimentation at a water to soil mass ratio
153 of 1 to 8 to obtain WDC suspension. All samples were extracted and analyzed in triplicate. In brief,
154 10 g soil subsamples ($d < 8$ mm) were mixed with 20 mL deionized water and shaken on a horizontal
155 shaker at 150 rpm for 6.5 h. The suspension was then diluted four times with deionized water and
156 left to stand to allow sedimentation (approximately 6 min, according to Stokes' law, particle density
157 was assumed as 1.5 g cm^{-3}) to remove the particles $> 20 \text{ }\mu\text{m}$ ^{10,42}. Then, the supernatant was
158 transferred into a 25-mL centrifuge tube, and the suspension ($< 20 \text{ }\mu\text{m}$) was centrifuged at 4000 rpm
159 for approximately 7 min. The centrifugation time was calculated according to Hathaway (1956) to
160 obtain WDC with a particle size of $< 500 \text{ nm}$ in the supernatant^{43,44}. Irrigation experiments with
161 undisturbed mesocosm soil columns demonstrated that the leached colloids had a maximum size of
162 400 nm ²⁶. For additional details see supplementary information (section S1). In addition, dynamic
163 light scattering (DLS) measurements (Malvern Nano-ZS, Malvern Panalytical, UK) were performed
164 on the separated WDC samples to verify the effectiveness of the size fractionation, and the z-average
165 of diameter was calculated based on the intensity distribution (Table S6)^{43,19}.

166 The truly dissolved elemental fractions were determined by ultrafiltration using a molecular
167 weight cut off of 3 kDa (Millipore, USA). 15 mL of WDC suspension were centrifuged at 4000 g
168 for 15 min. The permeate was collected and analyzed by ICP-MS and OCD for P, Fe, Al, Si, Ca, Mg
169 and organic carbon.

170 **Asymmetric Flow Field Flow Fractionation**

171 Size resolved elemental characterization of the colloidal fractions in the extracted WDCs was
172 achieved by AF4 (AF2000, Postnova Analytics, Landsberg, Germany) using a 1 kDa PES membrane,
173 1 mL injection volume, 20 min focusing time and a separation time of 91 min including a cross flow
174 gradient from 2.5 mL min⁻¹ down to zero. The AF4 was coupled online to a UV-vis detector
175 (Postnova Analytics), a DLS detector (Malvern Nano-ZS, Malvern Panalytical, UK) and a C_{org}
176 detector (OCD; DOC laboratory Dr. Huber, Germany) for quantification of the particulate organic
177 carbon using multipoint external calibration and determination of the particle size. In parallel, the
178 same AF4 method was run with ICP-MS detection (Agilent 7500, Agilent Technologies, Japan) for
179 quantification of the particulate elemental concentrations monitoring ³¹P, ⁵⁶Fe, ²⁷Al, ²⁸Si, ⁴⁴Ca and
180 ²⁴Mg using He collision cell mode. A post channel calibration approach was applied using Rh as the
181 internal standard which was developed and validated in our previous work^{45,46}. Latex particles were
182 analyzed with the same AF4 method as size markers for the obtained colloidal fractions (Figure S2).
183 Further experimental details are given in the supporting information (section S2, Table S7 and Table
184 S8).

185 **Colloidal Phosphorus Saturation.** Similar to the definition of soil P saturation (DPS)⁴⁷, the
186 colloidal P saturation (DPS_{coll}) was used to assess the P adsorption capacity of soil colloids at 15
187 sites in Zhejiang Province. The DPS_{coll} was calculated using the following formula:

$$188 \quad DPS_{coll} = \frac{P_{coll}}{Fe_{coll} + Al_{coll}} \times 100\%$$

189 where Fe_{coll}, Al_{coll}, and P_{coll} denote the Fe, Al, and P contents in the colloid, respectively, and the unit
190 of the Fe_{coll}, Al_{coll}, and P_{coll} is mmol kg⁻¹.

191 **Statistical Analysis.** Statistical analysis was performed using SPSS statistical software

192 package (SPSS Inc. Chicago, USA). A least significant difference (LSD) test at $P = 0.05$ level was
193 used to determine significant differences among the results of different fertilization treatments.
194 Origin 20.0 software (OriginLab Corp., US) was used for graphical processing. Pearson correlation
195 analysis and linear fitting were used to identify the relationships between nano-, fine- and medium-
196 colloidal P, and other colloidal and soil parameters.

197 ■ RESULTS

198 **Soil colloidal composition under varying agricultural geo-landscapes.** The fractograms
199 indicated that all 15 soil samples consisted of 2 or 3 size fractions as observed by the monitored
200 elemental peaks with similar elution times between samples (Figure 1). The first peak contained the
201 smaller nano colloids (approximately 0.6–25 nm; lower limit calculated from the membrane pore
202 size of 1 kDa); the second peak was assigned to larger nano colloids and fine colloids (approximately
203 25–160 nm, fine colloidal fraction); the third peak (after release of the cross flow) was related to
204 medium colloids (approximately 160–500 nm). In all H, all M and the L1 soils, all three fractions
205 were observed, and generally dominated by the fine colloidal fraction except for L1. However, in
206 L2–L5, only the first and third fraction was detected.

207 The soil colloidal P (0.6–500 nm) can be divided into three groups: high (H1–H5, 3583–6142
208 $\mu\text{g kg}^{-1}$), medium (M1–M5, 859–2612 $\mu\text{g kg}^{-1}$), and low (L1–L5, 514–653 $\mu\text{g kg}^{-1}$) (Figure 2, Table
209 1). The medium and high-level groups originated from the Basins and Mountains of Central and
210 Southeast, which were characterized by very low P contents in the nano- and medium-colloidal size
211 fractions, however, contained high amount of P in the fine-colloidal fraction. The fine-colloidal P
212 content of the high-level group accounted for 77–89% of the total determined colloidal P content

213 (Figure 2, Table 1). Peaks of fractograms were much less clear for northern plains soils, which
214 comprised the low-level colloidal P group (Figure 2). The fine- and medium-colloidal P here only
215 accounted for 28–39% and 35–53%, respectively, of the total colloidal P measured (Table 1).

216 In general, C_{org}, Si, Al, and Fe were the main constituent elements of soil fine and medium
217 colloidal fractions, while the C_{org} and Ca contents were most abundant of the monitored elements in
218 the soil nano colloidal fraction (Figure S3, Table 2). When comparing different colloidal size
219 fractions, the mean contents of C_{org}, Si, Al, and Fe (447, 164, 56.2 and 19.8 mg kg⁻¹, respectively),
220 were much higher than the mean Ca concentration (1.8 mg kg⁻¹) in the fine and medium colloidal
221 size (Figure S3, Table 2). However, in the nano colloidal fraction C_{org} and Ca were more abundant
222 with mean contents of 150.7 and 0.7 mg kg⁻¹ compared to the rather low mean contents of Fe and
223 Al of 0.2 mg kg⁻¹ and 0.5 mg kg⁻¹, respectively (Figure S3).

224

225 **Linkages of colloidal P with organic carbon at regional scale.** Colloidal Al, Fe, Ca, Si, and
226 C_{org} compositions were significantly correlated with colloidal P ($P < 0.05$). However, the fitting
227 results varied with the colloidal size fractions. For the nano colloidal fraction, only Ca and P
228 displayed a linear relationship (Figure 3). However, linear relationships were found between P and
229 C_{org}, Si, Al, Fe, and Ca in the fine colloidal fraction. In the medium colloidal fraction, there were
230 linear relationships between P and C_{org}, Si, Al, and Fe, with the strongest relationship between P and
231 Al (Figure 3).

232 The P saturation in the colloids showed that the L1–L5 had higher soil DPS_{coll} levels in the total
233 fractions, with a mean of ca. 20%, whereas it was only 1% in H1–H5 and M1–M5 (Table 1). In

234 addition, our analysis showed that DPS_{coll} was closely related to colloidal C_{org} (Figure 4). When the
235 C_{org} concentration was $< 200 \text{ mg kg}^{-1}$, the DPS_{coll} decreased sharply with the increase in the C_{org}
236 content, and when it exceeded 200 mg kg^{-1} , DPS_{coll} decreased gently with the increase of C_{org} , and
237 the scatter plot after log-transformation showed a negative correlation between C_{org} and DPS_{coll}
238 (Figure 4).

239

240 **Soil colloidal composition under different organic amendments input.** Carbon-based
241 fertilizer inputs did not affect the fractogram shapes of nano, fine, and medium colloids in the two
242 soils (Figures S4 and S5), and did not change the magnitude (medium level) of the colloidal P
243 distribution at the regional scale. The above assigned three size fractions were present in all
244 treatments. However, compared with the control, all treatments showed a (slight) increase in the
245 peak value (concentration), except for OFSB in which it decreased. Compared with CF, the OF
246 treatment mainly caused a significant increase of the C_{org} content of the nano colloidal fraction, but
247 Al, Fe, and Ca contents decreased in the fine colloids (Table S9, Figure S6). The BS treatment
248 significantly increased the C_{org} concentration in both nano and fine colloidal fractions ($P < 0.05$).
249 Furthermore, OFBS and BSSB significantly decreased the Al, Fe, and Ca contents in colloidal
250 fractions ($P < 0.05$).

251 Compared with CF at Site 1, the OF and OFSB treatments reduced the soil colloidal P content
252 (0.6–500 nm) by 33% and 43%, respectively, while at Site 2, BS increased colloidal P by 30% and
253 BSSB reduced colloidal P by 45% (Figure 5). In comparison with CF, the treatments of OF, OFBS,
254 and BSSB significantly reduced the concentration of fine colloidal P ($P < 0.05$), but had little effect

255 on nano colloidal P. However, the nano-colloidal P concentration of BS treatment was 50% higher
256 than that of CF, while the fine-colloidal P concentration of BS were 74%, 39%, and 178% higher
257 than those of CK, CF, and BSSB, respectively. In the medium colloidal fraction, no significant
258 differences of P content were detected between CK, CF, and OF/BS, however, in OFBS and BSSB
259 treatments, it was significantly lower than all other treatments. The truly dissolved P content of the
260 two soils significantly decreased after organic fertilizers application when compared to CF ($P <$
261 0.05), while the ratio between fine colloidal P and the truly dissolved P was higher in the two soils
262 with modified biochar (Figure S7).

263 ■ DISCUSSION

264 **Colloidal P formation as revealed by regional-scaled observation.** In this study, 2 or 3
265 colloidal fractions were found in 15 soils, which is similar to the findings in other soils or
266 streams^{20,26,43}. However, we found two distinct linkages of organic matter with the nano-colloidal
267 P and fine- and medium-colloidal P, respectively. Nano colloidal P is correlated with organic carbon
268 and Ca and most likely forming a complex of $C_{org}\text{-Ca-P}$, while fine colloidal and medium colloidal
269 P is correlated with clay mineral elements and likely to form a complex of $C_{org}\text{-clay-P}$.

270 Colloids (< 450 nm) extracted from soil or stream water usually contain nano-sized organic
271 matter (complex organic acids) in the size range of 1–5 nm¹⁹. Moreover, some macromolecular
272 degradation products and excreted (<100 nm) by microorganisms within soil, mainly comprising of
273 protein, DNA, and fat as well as extracellular polymeric substance (EPS), co-exist with P, which
274 was revealed by the high concentrations of P-monoesters and P-diester in the WDC extract
275 identified by NMR (Figure S8, Table S10). In most soils, nano-colloidal Fe and Al were present at

276 non-detectable levels, while Ca was present in significant amount along with organic carbon. This
277 is different from the finding¹⁹ by Jiang et al, 2015 that implied the binding mechanism of organic
278 matter and amorphous Fe or Al oxides in the nano colloidal fraction (<20 nm) of an acidic soil.
279 However, a recent study showed that binary humic acid (HA)-Ca complexes could incorporate P by
280 forming ternary HA-Ca-P complexes⁴⁸, and the P may also be bound in nano-colloidal minerals of
281 apatite^{49,50}. Furthermore, in calcareous soils, Ca²⁺ ions presumably bridged organic P and nano
282 colloidal negatively charged organic substances with carboxyl or phenolic groups^{42,51,52}. Therefore,
283 we assume that nano colloids are dominated by organic compounds, and that their small-sized acid
284 moieties may form stable nanoparticles through the bridging of Ca²⁺ ions. This is also supported by
285 a strongly positive correlation with nano-colloidal Ca and P, but non-significant correlations with
286 nano-colloidal Fe, Al, or Si (Figure 3). However, the fact that there were little differences between
287 the C_{org} content in nano colloids of the soils, and C_{org}/P and Ca/P were basically fixed at
288 approximately 4000:1 and 4:1, respectively (Table 2 and S10), may indicate that the binding capacity
289 of P to nano colloids was limited.

290 The fine colloidal fraction with the highest intensity of the three separated size fractions in most
291 soils (H1–H5 and M1–M5) contains large amounts of C_{org}, Si, Al, and Fe, and this size fraction is
292 usually formed from stable organic-inorganic composite colloids consisting of clay minerals, Fe/Al
293 (hydr)oxides and organic matter^{19,53}. This was revealed by the fixed molar ratio of Si/Al (1:0.5)
294 elements in the colloids (Table S11), which was consistent with the composition of 2:1 clay
295 minerals^{19,54,55}, and the fact that the soil clay minerals in the Zhejiang area contains more muscovite
296 and montmorillonite (Figure S9)⁵⁶. Considering the relatively constant Fe/Si molar ratio

297 (approximately 0.1:1; Table S11), the clay minerals in this area may have the fixed ratio of
298 isomorphic substitution between Fe and Al⁵⁷, and/or Fe oxides form complexes with clay minerals
299 and organic matter, respectively. The medium colloidal fraction with a lower intensity, represented
300 the larger WDC, but may have included small aggregates of nano and fine colloids¹⁹ and occasional
301 residual particles of sizes > 500 nm. In contrast to H1–H5 and M1–M5 soils, the fine colloidal
302 fraction of L1–L5 soils is missing, which may be related to the lower clay content of these soils
303 (Table S1). Some studies reported that the soil colloid content is closely related to the clay mineral
304 content^{58,59}, which presumably immobilizes the P in the soil through adsorption, ligand exchange,
305 and precipitation^{19,60–61}. The fine-colloidal P dominated by C_{org}, Si, Fe, and Al, accounted for 80%
306 of the total colloidal P for H1–H5 and M1–M5 and 36% of total colloidal P for L1–L5. Note, Ca²⁺
307 may also participate in the fine colloid formation process, connecting colloids and organic matter^{42,62}.
308 In addition, Ca²⁺ may play an important role in bridging inorganic P and organic P on clay minerals
309 accompanied by organic matter⁴⁵.

310 The P saturation in the colloids showed that the L1–L5 had significantly higher soil DPS_{coll}
311 levels than H1–H5 and M1–M5 (Table 1). Furthermore, there was a negative correlation between
312 the DPS_{coll} and C_{org} concentrations (Figure 4). Some studies also confirmed that when the surface
313 adsorption sites of soil are occupied by a large amount of organic substances, the adsorption capacity
314 of clay particles for phosphate ions will be weakened^{63–64}. The organic carbon compounds with
315 competitive inhibition of P sorption are usually derived from low molecular weight organic acids
316 (LOAs), humic and fulvic acids, and organic leachates⁶⁵. Therefore, the degree of P saturation in
317 fine and medium colloids can directly reflect the amount of soil P carried by the colloids which can

318 be used in the future to predict the P retention capacity of soil colloids and the risk of P loss. It is
319 worth noting that in nano colloids fraction, the adsorption mechanism of P was not related to Fe and
320 Al, but rather to the complexation of Ca and organic matter. Therefore, DPS_{coll} cannot be simply
321 used for the prediction of nano-colloidal P in the soils studied.

322 Colloidal P in the fractograms of the agricultural soil colloids revealed spatial distribution
323 characteristics at the regional scale (Table 1). This also may be subject to the differences in soil
324 mineralogy and organic C storage. A study in the subtropical forests found that soil organic C was
325 highly correlated with P sorption index⁶⁶, and many organic P compounds sorb strongly to positively
326 charged mineral surfaces of amorphous Al and Fe oxide and the edge of clay minerals⁶⁷. The
327 subtropical monsoon affected humid climate zone in the middle and southern Zhejiang where the
328 soil is rich in iron and aluminum and lower in C storage (Table S1)⁵⁶, resulting in the existence of a
329 high-medium level group of colloidal P. Soils on the Northern Plain usually have lower
330 aluminization and obvious accretion layers⁵⁶ and show a higher C storage and clay content (Table
331 S1), resulting in the low level group of colloidal P. This pattern assignment also basically proves our
332 first hypothesis that specific distribution patterns of colloidal P occur at regional scale. However, in
333 fact, the terrain topography in Zhejiang Province is complicated⁵⁶, and the current classification of
334 colloidal P fractions in this region is therefore still relatively coarse. Note, in view of the high
335 instrumental and time effort of the AF4 technology with ICP-MS detection for testing a large number
336 of samples, an initial set of 15 samples (3 repetitions each) was investigated in detail in this study to
337 achieve a basic characterization at the regional scale. A further study in the future is needed to
338 increase the sampling site density and evaluate the colloidal P distribution pattern in higher spatial

339 and possibly even temporal resolution at the regional scale.

340

341 **Effects of organic fertilizer inputs on soil colloidal P.** Our study found that 2 years of
342 differential fertilization had no significant effect on the fractogram shape (i.e., magnitude and
343 composition) of nano- and fine-colloidal sized particles isolated from two soils. Therefore, we
344 conclude that the soil textures and the contents of the particulate matrix elements (i.e., C_{org} , Fe, Al,
345 Si, Ca) affect the composition, distribution, and morphology of soil colloidal fractions, while the
346 difference in the type of fertilization and carbon inputs affects the concentration of compounds (i.e.,
347 P) adsorbed by colloids. However, the ability of colloids in different soils to carry P has been
348 determined by soil conditions, which is supported by the concept of DPS_{coll} proposed above.
349 Therefore, the first step to investigate the colloidal loss potential of a special type of soil is to
350 understand its organic and mineral phase composition. This is an important prerequisite for
351 formulating a P management strategy. Understanding this premise is of great significance to the
352 management of P loss in the agricultural field at different regional scale.

353 Indeed, fertilization regimes significantly affected the soil nano-colloidal P and fine-colloidal
354 P concentrations in a particular type of soil. Specifically, compared with the control, the application
355 of chemical fertilizer enhanced the P saturation of fine colloids by increasing the phosphate
356 concentration, and boosted the nano-colloidal and fine-colloidal P contents in the soil. The strong
357 correlation between the truly dissolved P or available P and colloidal P further confirmed the
358 occurrence of that process (Figure S10). Compared with CF, when organic fertilizer replaced 30%
359 of the chemical P, the colloidal P content significantly decreased. This was mainly due to the increase

360 of organic matter, which sheltered the colloidal adsorption sites^{63,64}, and limited the chances of the
361 phosphate ions binding to colloids through adsorption, resulting in the reduction of the amount of
362 colloidal P. We further found that compared with the application of chemical fertilizers, organic
363 fertilizer and biochar applications increased the concentration of C_{org} in the soil colloids, but
364 decreased the concentrations of Fe and Al (Table S10). A study of a loam soil with long-term
365 application of poultry manure found that P was more likely to be associated with Ca than Fe or Al⁶⁸
366 and resulted in the conversion of relatively soluble Ca-P into more colloidal crystal phases. However,
367 when applying biogas slurry instead of 30% chemical P, the amounts of nano-colloidal and fine
368 colloidal P in the soil increased significantly (Figure 5). This may be due to the biogas slurry itself
369 containing a large amount of organic colloidal P, which is bound to clay colloids or exist in the nano
370 P form once entering the soil²⁹. Compared with CF, OF, and BS, the application of modified biochar
371 significantly reduced the amount of colloidal P in the soil. The two explanations for this are: 1) P
372 adsorption on biochar³³, and 2) the modified biochar promotes the formation of soil aggregates⁶⁹.
373 Overall, more systematic field experiments including runoff and leaching losses are warranted to
374 investigate and verify the effect of fertilization on the morphology and migration of colloidal P.


375 ■ ASSOCIATED CONTENT

376 Supporting Information


377 Sections S1-S3; Figures S1–S10; Tables S1–S11

378 ■ AUTHOR INFORMATION


379 **Corresponding Author**


380 **Xinqiang Liang** – Key Laboratory of Environment Remediation and Ecological Health, Ministry
381 of Education, College of Environmental and Resources Sciences, Zhejiang University,
382 Hangzhou 310058, China.  <https://orcid.org/0000-0002-3521-9761>
383 Tel & fax: 86-0571- 88982809
384 Email : liang410@zju.edu.cn


385 **Authors**

386 **Fayong Li** – Key Laboratory of Environment Remediation and Ecological Health, Ministry of
387 Education, College of Environmental and Resources Sciences, Zhejiang University,
388 Hangzhou 310058, China.  <https://orcid.org/0000-0002-7893-9451>

389 **Qian Zhang** – Institute of Bio- and Geosciences, Agrosphere (IBG-3), Forschungszentrum Jülich
390 GmbH, 52425, Jülich, Germany; Institute for Environmental Research, Biology 5, RWTH
391 Aachen University, Worringerweg 1, 52074 Aachen, Germany.

392 **Erwin Klumpp** – Institute of Bio- and Geosciences, Agrosphere (IBG-3), Forschungszentrum
393 Jülich GmbH, 52425, Jülich, Germany.  <https://orcid.org/0000-0002-4810-9414>

394 **Roland Bol** – Institute of Bio- and Geosciences, Agrosphere (IBG-3), Forschungszentrum Jülich
395 GmbH, 52425, Jülich, Germany; School of Natural Sciences, Environment Centre Wales,
396 Bangor University, Bangor, LL57 2UW, U.K.  <https://orcid.org/0000-0003-3015-7706>

397 **Volker Nischwitz** – Central Institute for Engineering, Electronics and Analytics, Analytics (ZEA-
398 3), Forschungszentrum Juelich, 52425 Juelich, Germany.  <https://orcid.org/0000-0002-9261-3124>
399 9261-3124

400 **Zhuang Ge** – Northeast Key Laboratory of Conservation and Improvement of Cultivated Land
401 (Shenyang), Ministry of Agriculture, Shenyang Agricultural University, Shenyang, Liaoning
402 110866, China.

403 **Notes**

404 The authors declare no competing financial interest.

405 ■ **ACKNOWLEDGEMENTS**

406 We are grateful for grants from National Natural Science Foundation of China
407 (41522108;22076163); National Key Science and Technology Project: Water Pollution Control and
408 Treatment (2018ZX07208009); Natural Science Foundation of Zhejiang Province (LR16B070001).

409 We thank China Scholarship Council for providing scholarships to the students in this study.

410 **REFERENCES**

411 (1) He, S.; Li, F. Y.; Liang, X. Q.; Li, H.; Wang, S.; Jin, Y. B.; Liu, B. Y.; Tian, G. M. Window
412 Phase Analysis of Nutrient Losses from a Typical Rice-Planting Area in the Yangtze River
413 Delta Region of China. *Environ. Sci. Eur.* **2020**, *32* (1), 1–12. [https://doi.org/10.1186/s12302-](https://doi.org/10.1186/s12302-020-0291-0)
414 020-0291-0.

415 (2) Liang, X.; Jin, Y.; He, M.; Liu, Y.; Hua, G.; Wang, S.; Tian, G. Composition of Phosphorus
416 Species and Phosphatase Activities in a Paddy Soil Treated with Manure at Varying Rates.

- 417 *Agric. Ecosyst. Environ.* **2017**, *237*, 173–180. <https://doi.org/10.1016/j.agee.2016.12.033>.
- 418 (3) Bol, R.; Gruau, G.; Mellander, P. E.; Dupas, R.; Bechmann, M.; Skarbøvik, E.; Bieroza, M.;
419 Djodjic, F.; Glendell, M.; Jordan, P.; Van der Grift, B.; Rode, M.; Smolders, E.; Verbeeck,
420 M.; Gu, S.; Klumpp, E.; Pohle, I.; Fresne, M.; Gascuel-Oudou, C. Challenges of Reducing
421 Phosphorus Based Water Eutrophication in the Agricultural Landscapes of Northwest Europe.
422 *Front. Mar. Sci.* **2018**, *5* (AUG), 276. <https://doi.org/10.3389/fmars.2018.00276>.
- 423 (4) Solórzano, L.; Sharp, J. H. Determination of Total Dissolved Phosphorus and Particulate
424 Phosphorus in Natural Waters. *Limnol. Oceanogr.* **1980**, *25* (4), 754–758.
425 <https://doi.org/10.4319/lo.1980.25.4.0754>.
- 426 (5) Hens, M.; Merckx, R. The Role of Colloidal Particles in the Speciation and Analysis of
427 “Dissolved” Phosphorus. *Water Res.* **2002**, *36* (6), 1483–1492.
428 [https://doi.org/10.1016/S0043-1354\(01\)00349-9](https://doi.org/10.1016/S0043-1354(01)00349-9).
- 429 (6) Klitzke, S.; Lang, F.; Kaupenjohann, M. Increasing PH Releases Colloidal Lead in a Highly
430 Contaminated Forest Soil. *Eur. J. Soil Sci.* **2008**, *59* (2), 265–273.
431 <https://doi.org/10.1111/j.1365-2389.2007.00997.x>.
- 432 (7) Ran, Y.; Fu, J. M.; Sheng, G. Y.; Beckett, R.; Hart, B. T. Fractionation and Composition of
433 Colloidal and Suspended Particulate Materials in Rivers. *Chemosphere* **2000**, *41* (1–2), 33–
434 43. [https://doi.org/10.1016/S0045-6535\(99\)00387-2](https://doi.org/10.1016/S0045-6535(99)00387-2).
- 435 (8) Hartland, A.; Lead, J. R.; Slaveykova, V. I.; O’Carroll, D.; Valsami-Jones, E. The
436 Environmental Significance of Natural Nanoparticles | Learn Science at Scitable. *Nat. Educ.*
437 *Knowl.* **2013**, *4* (8), 7.

- 438 (9) Qafoku, N. P. Terrestrial Nanoparticles and Their Controls on Soil-/Geo-Processes and
439 Reactions. *Adv. Agron.* **2010**, *107* (C), 33–91. [https://doi.org/10.1016/S0065-2113\(10\)07002-](https://doi.org/10.1016/S0065-2113(10)07002-1)
440 1.
- 441 (10) Henderson, R.; Kabengi, N.; Mantripragada, N.; Cabrera, M.; Hassan, S.; Thompson, A.
442 Anoxia-Induced Release of Colloid- and Nanoparticle-Bound Phosphorus in Grassland Soils.
443 *Environ. Sci. Technol.* **2012**, *46* (21), 11727–11734. <https://doi.org/10.1021/es302395r>.
- 444 (11) Jiang, X.; Livi, K. J. T.; Arenberg, M. R.; Chen, A.; Chen, K. yue; Gentry, L.; Li, Z.; Xu, S.;
445 Arai, Y. High Flow Event Induced the Subsurface Transport of Particulate Phosphorus and
446 Its Speciation in Agricultural Tile Drainage System. *Chemosphere* **2021**, *263*, 128147.
447 <https://doi.org/10.1016/j.chemosphere.2020.128147>.
- 448 (12) Li, F. Y.; Liang, X. Q.; Liu, Z. W.; Tian, G. M. No-till with Straw Return Retains Soil Total
449 P While Reducing Loss Potential of Soil Colloidal P in Rice-Fallow Systems. *Agric. Ecosyst.*
450 *Environ.* **2019**, *286*, 106653. <https://doi.org/10.1016/j.agee.2019.106653>.
- 451 (13) Kaplan, D. I.; Bertsch, P. M.; Adriano, D. C.; Miller, W. P. Soil-Borne Mobile Colloids as
452 Influenced by Water Flow and Organic Carbon. *Environ. Sci. Technol.* **1993**, *27* (6), 1193–
453 1200. <https://doi.org/10.1021/es00043a021>.
- 454 (14) Baken, S.; Moens, C.; van der Grift, B.; Smolders, E. Phosphate Binding by Natural Iron-
455 Rich Colloids in Streams. *Water Res.* **2016**, *98*, 326–333.
456 <https://doi.org/10.1016/j.watres.2016.04.032>.
- 457 (15) Gottselig, N.; Bol, R.; Nischwitz, V.; Vereecken, H.; Amelung, W.; Klumpp, E. Distribution
458 of Phosphorus-Containing Fine Colloids and Nanoparticles in Stream Water of a Forest

- 459 Catchment. *Vadose Zo. J.* **2014**, *13* (7), vzj2014.01.0005.
460 <https://doi.org/10.2136/vzj2014.01.0005>.
- 461 (16) Bol, R.; Julich, D.; Brödlin, D.; Siemens, J.; Kaiser, K.; Dippold, M. A.; Spielvogel, S.; Zilla,
462 T.; Mewes, D.; von Blanckenburg, F.; Puhmann, H.; Holzmann, S.; Weiler, M.; Amelung,
463 W.; Lang, F.; Kuzyakov, Y.; Feger, K. H.; Gottselig, N.; Klumpp, E.; Missong, A.;
464 Winkelmann, C.; Uhlig, D.; Sohr, J.; von Wilpert, K.; Wu, B.; Hagedorn, F. Dissolved and
465 Colloidal Phosphorus Fluxes in Forest Ecosystems—an Almost Blind Spot in Ecosystem
466 Research. *J. Plant Nutr. Soil Sci.* **2016**, *179* (4), 425–438.
467 <https://doi.org/10.1002/jpln.201600079>.
- 468 (17) Liang, X.; Jin, Y.; Zhao, Y.; Wang, Z.; Yin, R.; Tian, G. Release and Migration of Colloidal
469 Phosphorus from a Typical Agricultural Field under Long-Term Phosphorus Fertilization in
470 Southeastern China. *J. Soils Sediments* **2016**, *16* (3), 842–853.
471 <https://doi.org/10.1007/s11368-015-1290-4>.
- 472 (18) Zarafshar, M.; Bazot, S.; Matinzadeh, M.; Bordbar, S. K.; Roustaei, M. J.; Kooch, Y.; Enayati,
473 K.; Abbasi, A.; Negahdarsaber, M. Do Tree Plantations or Cultivated Fields Have the Same
474 Ability to Maintain Soil Quality as Natural Forests? *Appl. Soil Ecol.* **2020**, *151*, 103536.
475 <https://doi.org/10.1016/j.apsoil.2020.103536>.
- 476 (19) Jiang, X.; Bol, R.; Nischwitz, V.; Siebers, N.; Willbold, S.; Vereecken, H.; Amelung, W.;
477 Klumpp, E. Phosphorus Containing Water Dispersible Nanoparticles in Arable Soil. *J.*
478 *Environ. Qual.* **2015**, *44* (6), 1772–1781. <https://doi.org/10.2134/jeq2015.02.0085>.
- 479 (20) Missong, A.; Bol, R.; Nischwitz, V.; Krüger, J.; Lang, F.; Siemens, J.; Klumpp, E. Phosphorus

- 480 in Water Dispersible-Colloids of Forest Soil Profiles. *Plant Soil* **2018**, 427 (1–2), 71–86.
481 <https://doi.org/10.1007/s11104-017-3430-7>.
- 482 (21) Gu, S.; Gruau, G.; Dupas, R.; Jeanneau, L. Evidence of Colloids as Important Phosphorus
483 Carriers in Natural Soil and Stream Waters in an Agricultural Catchment. *J. Environ. Qual.*
484 **2020**, 49 (4), 921–932. <https://doi.org/10.1002/jeq2.20090>.
- 485 (22) Jiang, X.; Bol, R.; Cade-Menun, B. J.; Nischwitz, V.; Willbold, S.; Bauke, S.; Vereecken, H.;
486 Amelung, W.; Klumpp, E. Colloid-Bound and Dissolved Phosphorus Species in Topsoil
487 Water Extracts along a Grassland Transect from Cambisol to Stagnosol. *Biogeosciences* **2017**,
488 14 (5), 1153–1164. <https://doi.org/10.5194/bg-14-1153-2017>.
- 489 (23) Giddings, J. C.; Yang, F. J. F.; Myers, M. N. Flow Field-Flow Fractionation: A Versatile New
490 Separation Method. *Science* (80-.). **1976**, 193 (4259), 1244–1245.
491 <https://doi.org/10.1126/science.959835>.
- 492 (24) Gottselig, N.; Amelung, W.; Kirchner, J. W.; Bol, R.; Eugster, W.; Granger, S. J.; Hernández-
493 Crespo, C.; Herrmann, F.; Keizer, J. J.; Korkiakoski, M.; Laudon, H.; Lehner, I.; Löfgren, S.;
494 Lohila, A.; Macleod, C. J. A.; Mölder, M.; Müller, C.; Nasta, P.; Nischwitz, V.; Paul-Limoges,
495 E.; Pierret, M. C.; Pilegaard, K.; Romano, N.; Sebastià, M. T.; Stähli, M.; Voltz, M.;
496 Vereecken, H.; Siemens, J.; Klumpp, E. Elemental Composition of Natural Nanoparticles and
497 Fine Colloids in European Forest Stream Waters and Their Role as Phosphorus Carriers.
498 *Global Biogeochem. Cycles* **2017**, 31 (10), 1592–1607.
499 <https://doi.org/10.1002/2017GB005657>.
- 500 (25) Jiang, X.; Bol, R.; Willbold, S.; Vereecken, H.; Klumpp, E. Speciation and Distribution of P

- 501 Associated with Fe and Al Oxides in Aggregate-Sized Fraction of an Arable Soil.
502 *Biogeosciences* **2015**, *12* (21), 6443–6452. <https://doi.org/10.5194/bg-12-6443-2015>.
- 503 (26) Missong, A.; Holzmann, S.; Bol, R.; Nischwitz, V.; Puhlmann, H.; v. Wilpert, K.; Siemens,
504 J.; Klumpp, E. Leaching of Natural Colloids from Forest Topsoils and Their Relevance for
505 Phosphorus Mobility. *Sci. Total Environ.* **2018**, *634*, 305–315.
506 <https://doi.org/10.1016/j.scitotenv.2018.03.265>.
- 507 (27) Liu, X. P.; Bi, Q. F.; Qiu, L. L.; Li, K. J.; Yang, X. R.; Lin, X. Y. Increased Risk of Phosphorus
508 and Metal Leaching from Paddy Soils after Excessive Manure Application: Insights from a
509 Mesocosm Study. *Sci. Total Environ.* **2019**, *666*, 778–785.
510 <https://doi.org/10.1016/j.scitotenv.2019.02.072>.
- 511 (28) Weyers, E.; Strawn, D. G.; Peak, D.; Baker, L. L. Inhibition of Phosphorus Sorption on
512 Calcite by Dairy Manure-Sourced DOC. *Chemosphere* **2017**, *184*, 99–105.
513 <https://doi.org/10.1016/j.chemosphere.2017.05.141>.
- 514 (29) Niyungeko, C.; Liang, X.; Liu, C.; Liu, Z. wen; Sheteiwy, M.; Zhang, H.; Zhou, J.; Tian, G.
515 Effect of Biogas Slurry Application Rate on Colloidal Phosphorus Leaching in Paddy Soil: A
516 Column Study. *Geoderma* **2018**, *325*, 117–124.
517 <https://doi.org/10.1016/j.geoderma.2018.03.036>.
- 518 (30) Niyungeko, C.; Liang, X.; Liu, C.; Zhou, J.; Chen, L.; Lu, Y.; Tiimub, B. M.; Li, F. Effect of
519 Biogas Slurry Application on Soil Nutrients, Phosphomonoesterase Activities, and
520 Phosphorus Species Distribution. *J. Soils Sediments* **2020**, *20* (2), 900–910.
521 <https://doi.org/10.1007/s11368-019-02435-y>.

- 522 (31) Kim, J. A.; Vijayaraghavan, K.; Reddy, D. H. K.; Yun, Y. S. A Phosphorus-Enriched Biochar
523 Fertilizer from Bio-Fermentation Waste: A Potential Alternative Source for Phosphorus
524 Fertilizers. *J. Clean. Prod.* **2018**, *196*, 163–171. <https://doi.org/10.1016/j.jclepro.2018.06.004>.
- 525 (32) Hosseini, S. H.; Liang, X.; Niyungeko, C.; Miaomiao, H.; Li, F.; Khan, S.; Eltohamy, K. M.
526 Effect of Sheep Manure-Derived Biochar on Colloidal Phosphorus Release in Soils from
527 Various Land Uses. *Environ. Sci. Pollut. Res.* **2019**, *26* (36), 36367–36379.
528 <https://doi.org/10.1007/s11356-019-06762-y>.
- 529 (33) Li, F. Y.; Liang, X. Q.; Niyungeko, C.; Sun, T.; Liu, F.; Arai, Y. Effects of Biochar
530 Amendments on Soil Phosphorus Transformation in Agricultural Soils. *Adv. Agron.* **2019**,
531 *158*, 131–172. <https://doi.org/10.1016/bs.agron.2019.07.002>.
- 532 (34) Zhang, H.; Chen, C.; Gray, E. M.; Boyd, S. E.; Yang, H.; Zhang, D. Roles of Biochar in
533 Improving Phosphorus Availability in Soils: A Phosphate Adsorbent and a Source of
534 Available Phosphorus. *Geoderma* **2016**, *276*, 1–6.
535 <https://doi.org/10.1016/j.geoderma.2016.04.020>.
- 536 (35) Wang, S.; Li, T.; Zheng, Z. Distribution of Microbial Biomass and Activity within Soil
537 Aggregates as Affected by Tea Plantation Age. *Catena* **2017**, *153*, 1–8.
538 <https://doi.org/10.1016/j.catena.2017.01.029>.
- 539 (36) ISO11277. *Soil Quality – Determination of Particle Size Distribution in Mineral Soil*
540 *Material – Method by Sieving and Sedimentation*; International Organization for
541 Standardization: Geneva, Switzerland, 1998.
- 542 (37) Sumner, M. E.; Miller, W. P. Cation Exchange Capacity and Exchange Coefficients. *Methods*

- 543 *Soil Anal. Part 3 Chem. Methods* **2018**, 1201–1229.
544 <https://doi.org/10.2136/sssabookser5.3.c40>.
- 545 (38) Walker, T. W.; Adams, A. F. R. Studies on Soil Organic Matter: I. Influence of Phosphorus
546 Content of Parent Materials on Accumulations of Carbon, Nitrogen, Sulfur, and Organic
547 Phosphorus in Grassland Soils. *Soil Sci.* **1958**, 85 (6), 307–318.
548 <https://doi.org/10.1097/00010694-195806000-00004>.
- 549 (39) Schwertmann, U. The Differentiation of Iron Oxides in Soils by Extraction with NH₄-
550 Oxalates Solution. *Zeitschrift für Pflanzenernährung und Bodenkd.* **1964**, 105, 194–202.
- 551 (40) Olsen, S. R.; Sommers, L. E. Phosphorus. In *Methods of Soil Analysis Part 2 Chemical and*
552 *Microbiological Properties*; Page, A. L., Ed.; American Society of Agronomy, Soil Science
553 Society of America: Madison, 1982; pp 403–430.
- 554 (41) Séquaris, J. M.; Lewandowski, H. Physicochemical Characterization of Potential Colloids
555 from Agricultural Topsoils. In *Colloids and Surfaces A: Physicochemical and Engineering*
556 *Aspects*; 2003; Vol. 217, pp 93–99. [https://doi.org/10.1016/S0927-7757\(02\)00563-0](https://doi.org/10.1016/S0927-7757(02)00563-0).
- 557 (42) Wang, L.; Missong, A.; Amelung, W.; Willbold, S.; Prietzel, J.; Klumpp, E. Dissolved and
558 Colloidal Phosphorus Affect P Cycling in Calcareous Forest Soils. *Geoderma* **2020**, 375,
559 114507. <https://doi.org/10.1016/j.geoderma.2020.114507>.
- 560 (43) Moradi, G.; Bol, R.; Trbojevic, L.; Missong, A.; Mörchen, R.; Fuentes, B.; May, S. M.;
561 Lehdorff, E.; Klumpp, E. Contrasting Depth Distribution of Colloid-Associated Phosphorus
562 in the Active and Abandoned Sections of an Alluvial Fan in a Hyper-Arid Region of the
563 Atacama Desert. *Glob. Planet. Change* **2020**, 185, 114170.

- 564 <https://doi.org/10.1016/j.gloplacha.2019.103090>.
- 565 (44) Hathaway, J. C. Procedure for Clay Mineral Analyses Used in the Sedimentary Petrology
566 Laboratory of the U.S. Geological Survey*. *Clay Miner.* **1956**, 3 (15), 8–13.
567 <https://doi.org/10.1180/claymin.1956.003.15.05>.
- 568 (45) Nischwitz, V.; Goenaga-Infante, H. Improved Sample Preparation and Quality Control for
569 the Characterisation of Titanium Dioxide Nanoparticles in Sunscreens Using Flow Field Flow
570 Fractionation On-Line with Inductively Coupled Plasma Mass Spectrometry. *J. Anal. At.*
571 *Spectrom.* **2012**, 27 (7), 1084–1092. <https://doi.org/10.1039/c2ja10387g>.
- 572 (46) Nischwitz, V.; Gottselig, N.; Missong, A.; Meyn, T.; Klumpp, E. Field Flow Fractionation
573 Online with ICP-MS as Novel Approach for the Quantification of Fine Particulate Carbon in
574 Stream Water Samples and Soil Extracts. *J. Anal. At. Spectrom.* **2016**, 31 (9), 1858–1868.
575 <https://doi.org/10.1039/c6ja00027d>.
- 576 (47) Zang, L.; Tian, G. M.; Liang, X. Q.; He, M. M.; Bao, Q. B.; Yao, J. H. Profile Distributions
577 of Dissolved and Colloidal Phosphorus as Affected by Degree of Phosphorus Saturation in
578 Paddy Soil. *Pedosphere* **2013**, 23 (1), 128–136. [https://doi.org/10.1016/S1002-](https://doi.org/10.1016/S1002-0160(12)60088-5)
579 [0160\(12\)60088-5](https://doi.org/10.1016/S1002-0160(12)60088-5).
- 580 (48) Audette, Y.; Smith, D. S.; Parsons, C. T.; Chen, W.; Rezanezhad, F.; Van Cappellen, P.
581 Phosphorus Binding to Soil Organic Matter via Ternary Complexes with Calcium.
582 *Chemosphere* **2020**, 260, 127624. <https://doi.org/10.1016/j.chemosphere.2020.127624>.
- 583 (49) Elliott, J. C. Structure and Chemistry of the Apatites and Other Calcium Orthophosphates.
584 *Stud. Org. Chem.* **1994**, 18, 94008066–94008066.

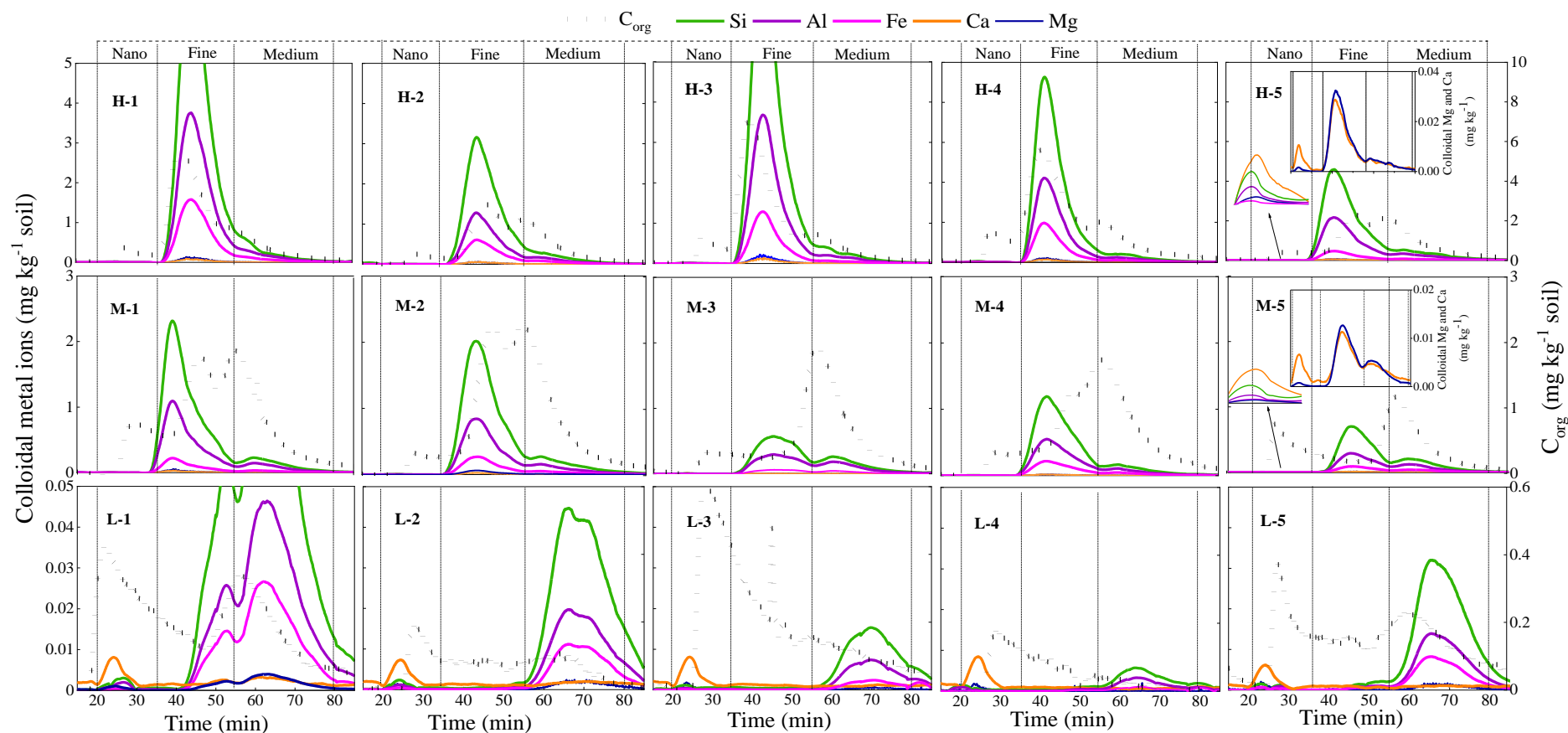
- 585 (50) Fu, B.; Sun, X.; Qian, W.; Shen, Y.; Chen, R.; Hannig, M. Evidence of Chemical Bonding to
586 Hydroxyapatite by Phosphoric Acid Esters. *Biomaterials* **2005**, *26* (25), 5104–5110.
587 <https://doi.org/10.1016/j.biomaterials.2005.01.035>.
- 588 (51) Lin, J.; Zhang, Z.; Zhan, Y. Effect of Humic Acid Preloading on Phosphate Adsorption onto
589 Zirconium-Modified Zeolite. *Environ. Sci. Pollut. Res.* **2017**, *24* (13), 12195–12211.
590 <https://doi.org/10.1007/s11356-017-8873-0>.
- 591 (52) Yang, X.; Chen, X.; Yang, X. Effect of Organic Matter on Phosphorus Adsorption and
592 Desorption in a Black Soil from Northeast China. *Soil Tillage Res.* **2019**, *187*, 85–91.
593 <https://doi.org/10.1016/j.still.2018.11.016>.
- 594 (53) Said-Pullicino, D.; Giannetta, B.; Demeglio, B.; Missong, A.; Gottselig, N.; Romani, M.; Bol,
595 R.; Klumpp, E.; Celi, L. Redox-Driven Changes in Water-Dispersible Colloids and Their
596 Role in Carbon Cycling in Hydromorphic Soils. *Geoderma* **2021**, *385*, 114894.
597 <https://doi.org/10.1016/j.geoderma.2020.114894>.
- 598 (54) Regelink, I. C.; Weng, L.; Koopmans, G. F.; van Riemsdijk, W. H. Asymmetric Flow Field-
599 Flow Fractionation as a New Approach to Analyse Iron-(Hydr)Oxide Nanoparticles in Soil
600 Extracts. *Geoderma* **2013**, *202–203*, 134–141.
601 <https://doi.org/10.1016/j.geoderma.2013.03.015>.
- 602 (55) Lazaratou, C. V.; Vayenas, D. V.; Papoulis, D. The Role of Clays, Clay Minerals and Clay-
603 Based Materials for Nitrate Removal from Water Systems: A Review. *Appl. Clay Sci.* **2020**,
604 *185*, 105377. <https://doi.org/10.1016/j.clay.2019.105377>.
- 605 (56) Zhejiang Soil Census Office. *Soil of Zhejiang*; Zhejiang Science and Technology Press:

- 606 Hangzhou, 1994.
- 607 (57) Kéri, A.; Dähn, R.; Marques Fernandes, M.; Scheinost, A. C.; Krack, M.; Churakov, S. V.
608 Iron Adsorption on Clays Inferred from Atomistic Simulations and X-Ray Absorption
609 Spectroscopy. *Environ. Sci. Technol.* **2020**, *54* (19), 11886–11893.
610 <https://doi.org/10.1021/acs.est.9b07962>.
- 611 (58) Laegdsmand, M.; De Jonge, L. W.; Moldrup, P. Leaching of Colloids and Dissolved Organic
612 Matter from Columns Packed with Natural Soil Aggregates. *Soil Sci.* **2005**, *170* (1), 13–27.
613 <https://doi.org/10.1097/00010694-200501000-00003>.
- 614 (59) Laegdsmand, M.; Moldrup, P.; De Jonge, L. W. Modelling of Colloid Leaching from
615 Unsaturated, Aggregated Soil. *Eur. J. Soil Sci.* **2007**, *58* (3), 692–703.
616 <https://doi.org/10.1111/j.1365-2389.2006.00854.x>.
- 617 (60) Bhatti, J. S.; Comerford, N. B.; Johnston, C. T. Influence of Oxalate and Soil Organic Matter
618 on Sorption and Desorption of Phosphate onto a Spodic Horizon. *Soil Sci. Soc. Am. J.* **1998**,
619 *62* (4), 1089–1095. <https://doi.org/10.2136/sssaj1998.03615995006200040033x>.
- 620 (61) Yaghi, N.; Hartikainen, H. Enhancement of Phosphorus Sorption onto Light Expanded Clay
621 Aggregates by Means of Aluminum and Iron Oxide Coatings. *Chemosphere* **2013**, *93* (9),
622 1879–1886. <https://doi.org/10.1016/j.chemosphere.2013.06.059>.
- 623 (62) Holzmann, S.; Missong, A.; Puhlmann, H.; Siemens, J.; Bol, R.; Klumpp, E.; Wilpert, K. von.
624 Impact of Anthropogenic Induced Nitrogen Input and Liming on Phosphorus Leaching in
625 Forest Soils. *J. Plant Nutr. Soil Sci.* **2016**, *179* (4), 443–453.
626 <https://doi.org/10.1002/jpln.201500552>.

- 627 (63) Celi, L.; Barberis, E. Abiotic Stabilization of Organic Phosphorus in the Environment. In
628 *Organic Phosphorus in the Environment*; Turner, B. L., Frossard, E., Baldwin, D. S., Eds.;
629 2004; pp 113–132. <https://doi.org/10.1079/9780851998220.0113>.
- 630 (64) Li, F. Y.; Yuan, C. yu; Yuan, Z. Q.; You, Y. jun; Hu, X. fei; Wang, S.; Li, G. yu. Bioavailable
631 Phosphorus Distribution in Alpine Meadow Soil Is Affected by Topography in the Tian Shan
632 Mountains. *J. Mt. Sci.* **2020**, *17* (2), 410–422. <https://doi.org/10.1007/s11629-019-5705-3>.
- 633 (65) Guppy, C. N.; Menzies, N. W.; Moody, P. W.; Blamey, F. P. C. Competitive Sorption
634 Reactions between Phosphorus and Organic Matter in Soil: A Review. *Australian Journal of*
635 *Soil Research*. 2005, pp 189–202. <https://doi.org/10.1071/SR04049>.
- 636 (66) Hou, E.; Chen, C.; Wen, D.; Liu, X. Relationships of Phosphorus Fractions to Organic Carbon
637 Content in Surface Soils in Mature Subtropical Forests, Dinghushan, China. *Soil Res.* **2014**,
638 *52* (1), 55–63. <https://doi.org/10.1071/SR13204>.
- 639 (67) Spohn, M. Increasing the Organic Carbon Stocks in Mineral Soils Sequesters Large Amounts
640 of Phosphorus. *Glob. Chang. Biol.* **2020**, *26* (8), 4169–4177.
641 <https://doi.org/10.1111/gcb.15154>.
- 642 (68) Sato, S.; Solomon, D.; Hyland, C.; Ketterings, Q. M.; Lehmann, J. Phosphorus Speciation in
643 Manure and Manure-Amended Soils Using XANES Spectroscopy. *Environ. Sci. Technol.*
644 **2005**, *39* (19), 7485–7491. <https://doi.org/10.1021/es0503130>.
- 645 (69) Zhou, J.; Liang, X.; Shan, S.; Yan, D.; Chen, Y.; Yang, C.; Lu, Y.; Niyungeko, C.; Tian, G.
646 Nutrient Retention by Different Substrates from an Improved Low Impact Development
647 System. *J. Environ. Manage.* **2019**, *238*, 331–340.

648 <https://doi.org/10.1016/j.jenvman.2019.03.019>.

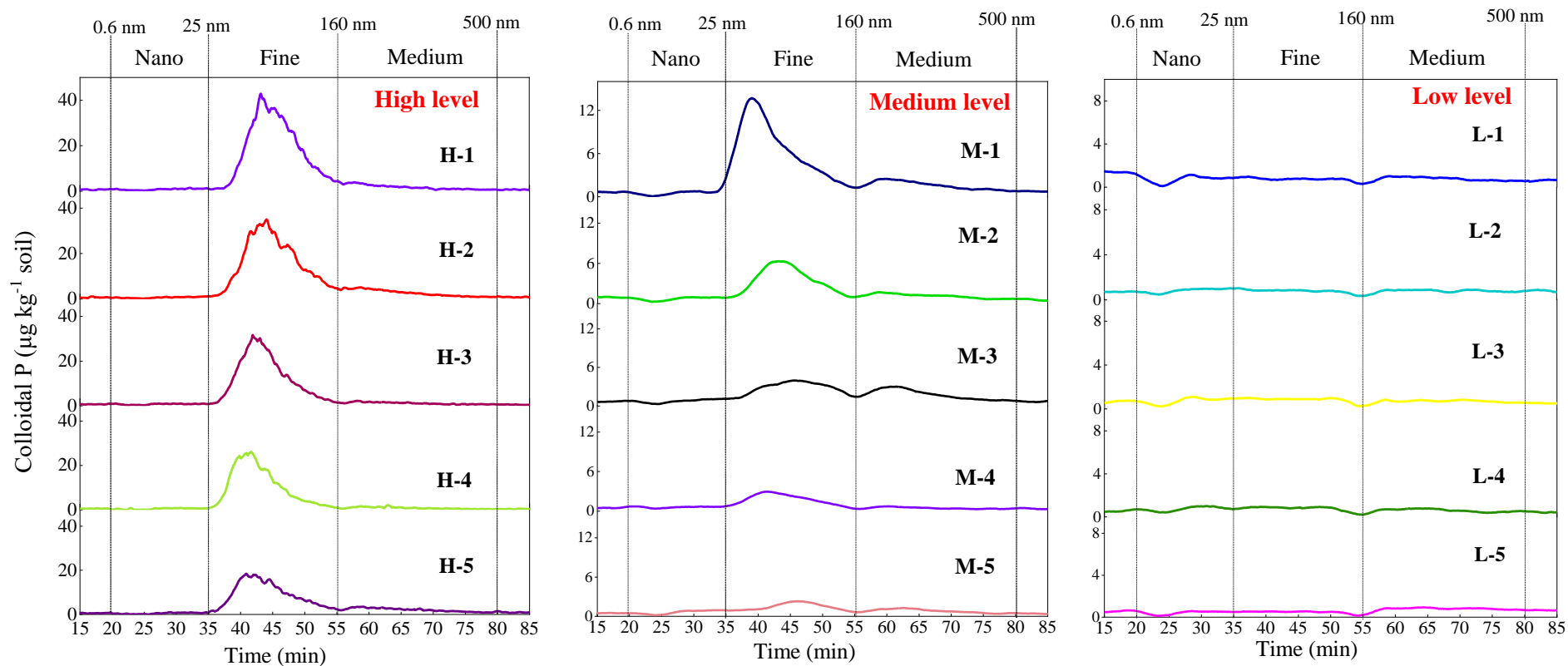
649



650

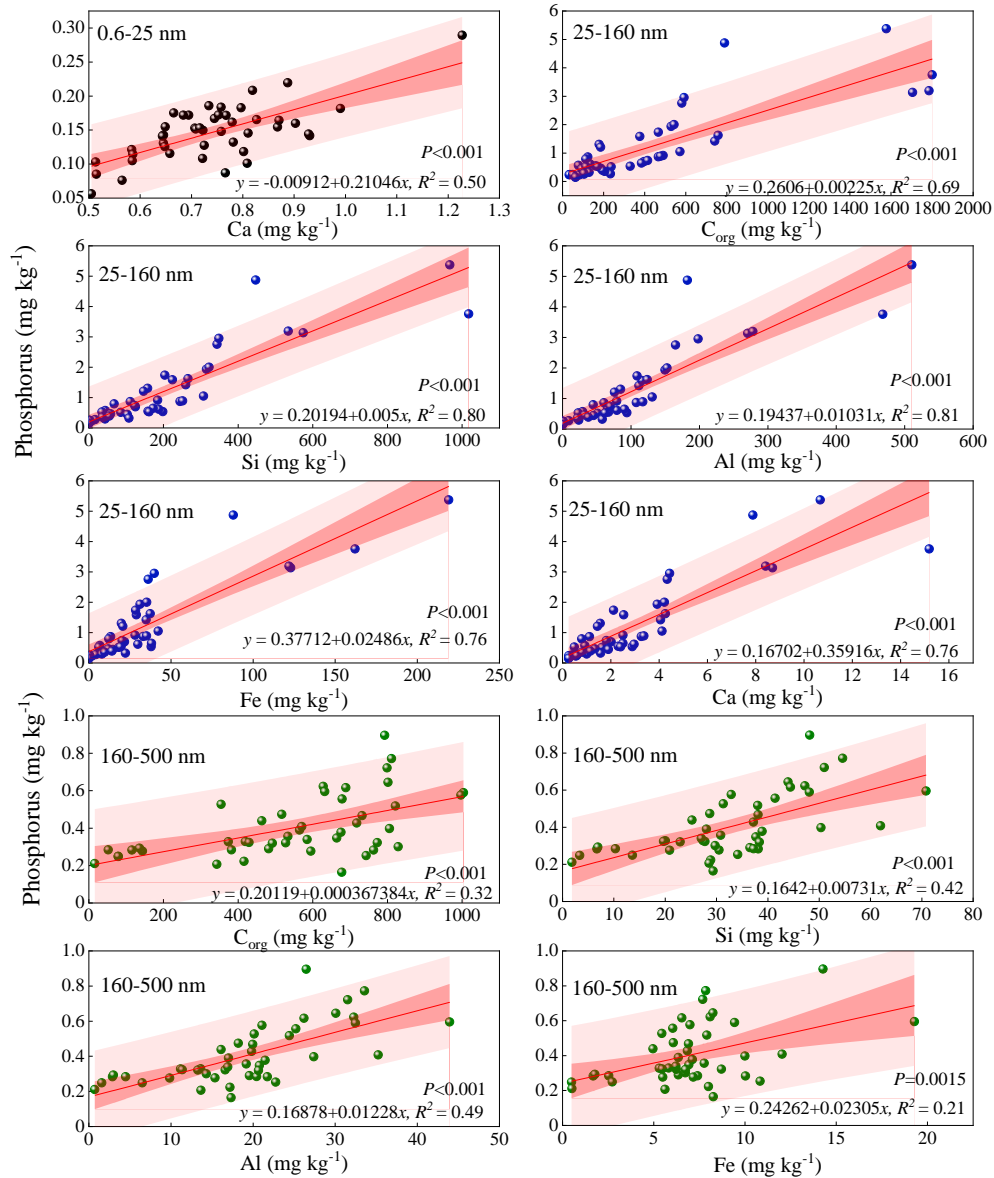
651 **Figure 1.** The fractogram of colloidal elements such as aluminum (Al), iron (Fe), silicon (Si), calcium (Ca), and organic carbon (C_{org}) in the soils at 15
 652 sites by Asymmetrical Flow Field Flow Fractionation (AF4) coupled with Inductively Coupled Plasma-Mass Spectrometer (ICP-MS) and Organic
 653 Carbon Detector (OCD). “Nano” is nano colloidal fraction (0.6–25 nm); “Fine” is fine colloidal fraction (25–160 nm); “Medium” is medium colloidal
 654 fraction (160–500 nm).

655



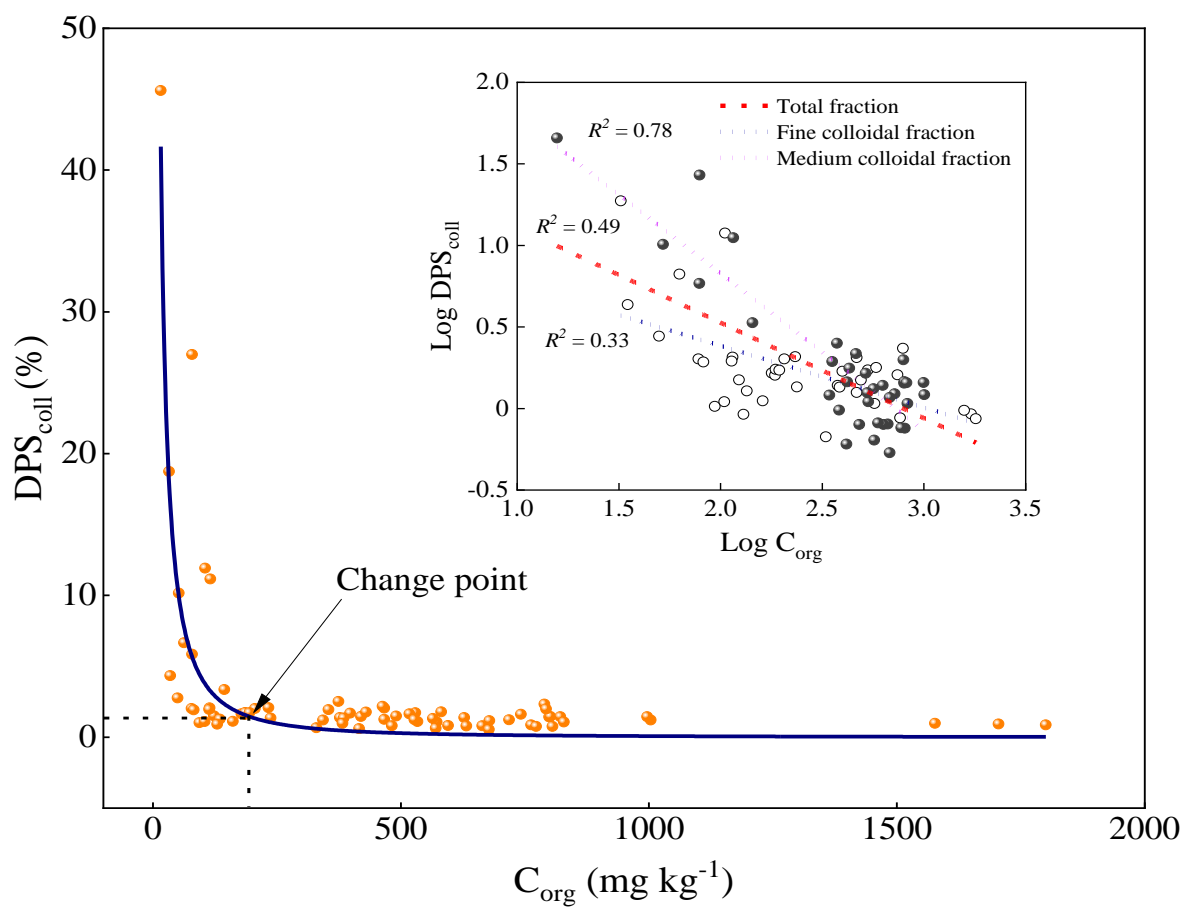
656

657 **Figure 2.** The fractogram of nano-colloidal (Nano), fine-colloidal (Fine) and medium-colloidal (Medium) phosphorus (P) in the 15 soils measured by
 658 Asymmetrical Flow Field Flow Fractionation (AF4) coupled with Inductively Coupled Plasma-Mass Spectrometer (ICP-MS). High, medium, and low
 659 levels indicate the peak level of colloidal P in the soils. Y-axis are scaled differently for the three figures.



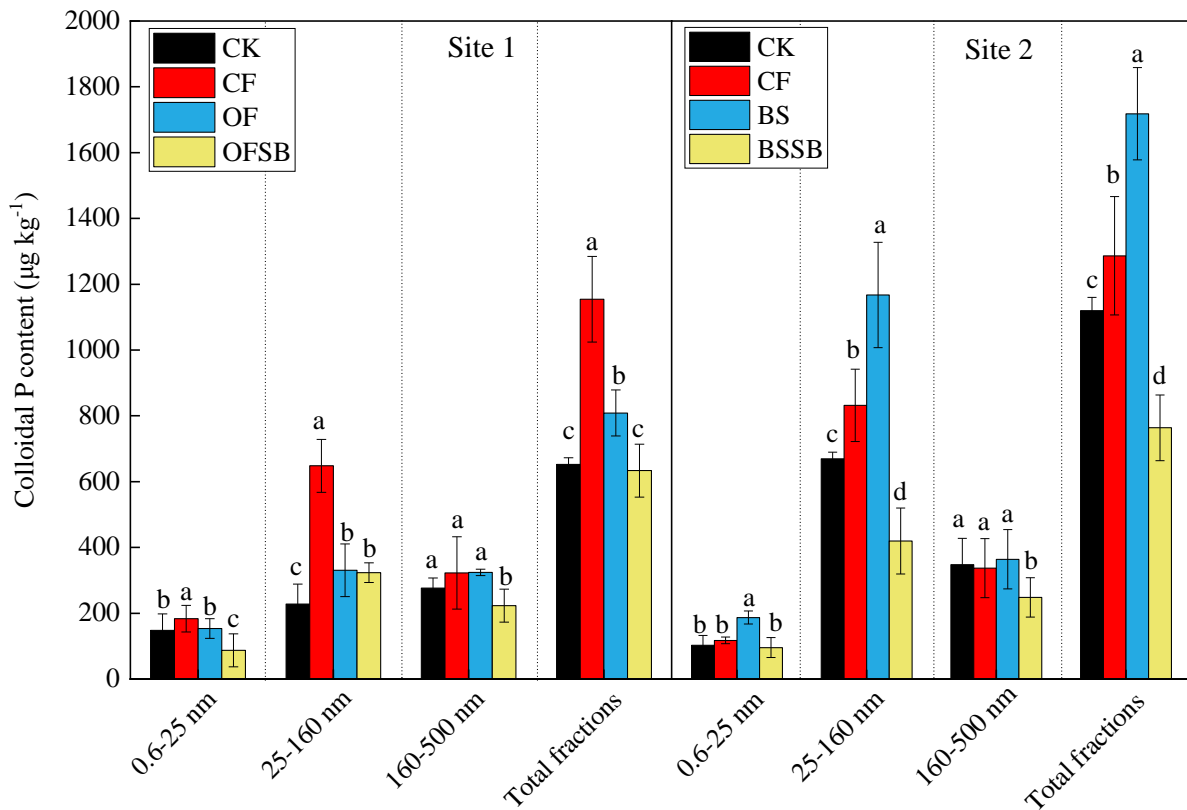
661

662 **Figure 3.** Nano- (0.6–25 nm), fine- (25–160 nm) and medium- (160–500 nm) colloidal phosphorus
 663 as a function of the content of other components in the same particle size fractions such as organic
 664 carbon (C_{org}), silicon (Si), aluminum (Al), iron (Fe), and calcium (Ca) (n=45)



665

666 **Figure 4.** The relationship between colloidal phosphorus saturation (DPS_{coll}) and colloidal organic
 667 carbon (C_{org}) (a), and the related linear fitting plot of DPS_{coll} and C_{org} after Log transformation (b).



669

670

671

672

673

674

675

676

Figure 5. Nano-, fine- and medium-colloidal phosphorus (P) content of different fractions in the soils at Site 1 and Site 2 under different fertilization treatments (n=3). CK represents control without fertilizer; CF represents conventional fertilization (chemical fertilizer); OF or BS represents organic fertilizer (sheep manure) or biogas slurry instead of 30% P application rate of chemical fertilizer, respectively; OFSB or BSSB represents organic fertilizer or biogas slurry + modified rice straw biochar instead of 30% P application rate of chemical fertilizer, respectively; Lowercase indicated significant difference between different fertilization treatments at $P < 0.05$ level.

677 **Table 1.** Colloidal phosphorus content and saturation (DPS_{coll}) of different particle size fractions in the 15 representative soils with different
 678 land-use types in Zhejiang Province, China.

Soils	Colloidal P content ($\mu\text{g kg}^{-1}$)				DPS_{coll} (%)		
	0.6–25 nm	25–160 nm	160–500 nm	Sum of fractions	25–160 nm	160–500 nm	Sum of fractions
H-1	172±11	5375±195	595±67	6142±214	0.8±0.1	1.0±0.1	0.8±0.2
H-2	142±25	4874±368	896±77	5912±359	1.9±0.3	2.4±0.1	2.0±0.2
H-3	155±13	3756±411	408±37	4318±498	0.6±0.1	0.9±0.1	0.6±0.3
H-4	103±9.0	3135±165	283±33	3603±189	0.8±0.1	0.9±0.1	0.9±0.2
H-5	108±10	2753±123	722±92	3583±189	1.3±0.0	2.0±0.1	1.4±0.2
M-1	121±11	1935±110	556±149	2612±99	1.0±0.1	1.7±0.2	1.2±0.1
M-2	150±24	1050±127	397±45	1597±145	0.6±0.0	1.1±0.3	0.8±0.2
M-3	160±29	863±102	623±77	1646±212	1.1±0.2	1.5±0.2	1.4±0.3
M-4	126±14	534±46	164±28	824±56	0.4±0.2	0.7±0.1	0.5±0.1
M-5	131±20	444±44	284±29	859±89	0.7±0.2	1.0±0.1	1.0±0.2
L-1	148±25	228±21	277±31	653±68	4.7±1.0	2.0±0.6	3.4±0.1
L-2	172±36	242±20	284±20	697±77	125±14	4.3±0.2	10±1.5
L-3	151±10	258±20	248±13	658±51	88±14	12±2.3	27±4.3
L-4	153±8.2	236±11	211±22	601±40	150±21	19±3.1	46±7.2
L-5	85±7.1	146±26	283±44	514±68	60±5.5	6.6±1.1	11±2.1

679

680

681 **Table 2.** The average (n=3) content of colloidal aluminum (Al), iron (Fe), silicon (Si), calcium (Ca), and organic carbon (C_{org}) content in
 682 the nano- (0.6–25 nm), fine- (25–160 nm), and medium- (160–500 nm) colloidal fractions of 15 soils determined by AF4-ICP-MS and
 683 AF4-OCD.

Sites	0.6–25 nm (mg kg ⁻¹)						25–160 nm (mg kg ⁻¹)						160–500 nm (mg kg ⁻¹)					
	C _{org}	Mg	Al	Si	Ca	Fe	C _{org}	Mg	Al	Si	Ca	Fe	C _{org}	Mg	Al	Si	Ca	Fe
H-1	166	0.10	0.75	1.2	0.69	0.31	1577	15	510	967	11	219	632	1.3	44	71	1.3	19
H-2	126	0.10	0.30	0.65	0.65	0.13	790	7.5	183	447	7.9	88	793	1.2	26	48	1.5	14
H-3	422	0.10	0.78	1.3	0.87	0.25	1800	23	468	1018	15	162	570	1.6	35	62	1.6	12
H-4	461	0.17	1.4	2.4	0.51	0.59	1705	12	271	574	8.7	123	763	1.0	22	38	1.0	10
H-5	123	0.09	0.24	0.49	0.72	0.06	582	4.9	165	343	4.3	36	799	1.0	32	51	1.0	7.7
M-1	218	0.14	1.7	3.1	0.58	0.42	529	5.5	150	315	3.9	31	679	1.0	25	41	0.77	6.0
M-2	97	0.08	0.20	0.46	0.72	0.07	572	9.2	131	307	4.1	42	806	2.0	27	50	1.0	10
M-3	92	0.12	0.15	0.31	0.90	0.04	123	1.1	61	111	1.1	13	628	0.7	32	47	0.78	8.1
M-4	103	0.07	0.30	0.57	0.65	0.12	330	2.9	94	198	2.9	38	679	0.62	17	29	0.84	8.3
M-5	161	0.07	0.15	0.36	0.65	0.06	94	2.0	45	103	1.9	15	382	1.0	20	37	1.1	7.4
L-1	112	0.08	0.16	0.29	0.76	0.04	82	0.30	3.3	7.4	0.55	1.9	144	0.83	9.9	21	0.79	5.5
L-2	42	0.07	0.09	0.21	0.68	0.04	35	0.02	0.14	0.36	0.38	0.06	52	0.46	4.5	10	0.57	2.5
L-3	165	0.09	0.04	0.15	0.71	0.02	105	0.03	0.24	0.45	0.37	0.04	80	0.11	1.6	3.4	0.36	0.50
L-4	44	0.09	0.02	0.09	0.72	0.01	32	0.01	0.12	0.29	0.26	0.04	16	0.02	0.73	1.8	0.24	0.52
L-5	78	0.09	0.06	0.12	0.51	0.07	63	0.03	0.15	0.30	0.25	0.13	116	0.28	2.9	6.7	0.34	1.7

684

685